

Viscoelastic Properties of Star-Shaped Polymers in Concentrated Solutions

Hirokazu Kajiura, Yoshiaki Ushiyama, Teruo Fujimoto,* and Mitsuru Nagasawa

Department of Synthetic Chemistry, Nagoya University, Chikusa-ku, Nagoya, Japan. Received January 10, 1978

ABSTRACT: Rheological parameters, i.e., the zero-shear viscosity η^0 and the limiting steady-state compliance J_e of three-armed, star-shaped polymers in concentrated solutions, were determined with a Weissenberg rheogoniometer. It was found that J_e of branched polymers shows a discontinuous transition from the moderate concentration region to the network region, just as J_e of linear polymers does. In the former region, J_e of star-shaped polymers is lower than that of linear polymers with the same molecular weight, and agrees with the predictions from the theory of Zimm and Kilb. In the latter region, it is proportional to inverse square concentration, as predicted from their network structure. Discussions are also given to η^0 of star-shaped polymers in comparison with that of linear polymers.

The rheological properties of homogeneous polymer systems, such as polymer solution or melt, may be described by two parameters, for example, the viscosity coefficient η and normal stress coefficient ψ_{12} (or steady-state compliance J_e). In the case of linear polymers,^{1,2} those parameters are well interpreted in terms of molecular characteristics in some molecular theories,³⁻⁹ at least in the linear region of deformation. In the case of branched polymers,¹⁰ however, our knowledge on their rheological properties is not yet satisfactory because of both experimental and theoretical difficulties. Theoretically, for example, zero-shear viscosity η^0 of branched polymers should be lower than that of corresponding linear polymers with the same molecular weights,¹¹⁻¹⁴ whereas clear enhancements in η^0 of some star-shaped polymers relative to those of linear polymers were reported by various authors.¹⁵⁻¹⁸ Moreover, although J_e of star-shaped polymers is lower than that of corresponding linear polymers with the same molecular weight at the limit of infinite dilution, as is predicted by theory,^{11,12,14} it was shown that J_e of some branched polymers is much higher than that of linear polymers in concentrated solutions and melt.¹⁸⁻²¹

The purpose of this work is to study the molecular weight and concentration dependence of rheological parameters of star-shaped polymers in moderately concentrated and concentrated solutions, using the samples prepared in a previous work.²² The samples have narrow molecular weight distributions and long branches. The purity of those samples is very high.

It is well known^{2,23-25} that the rheological properties of linear polymer solutions show quite different behavior in two concentration regions. In the moderately concentrated or Rouse region, the rheological properties of solutions are governed by the properties of individual molecules though there are some entanglements among molecules. Consequently, J_e in this region is proportional to M/C where M is the molecular weight of the linear polymer and C is the concentration. In the network or entanglement region, all molecules form a quasi-network structure. Consequently, J_e is proportional to $1/C^2$ and is independent of molecular weight. It is well known²⁶ that η^0 is proportional to $M^{3/4}$ in this region. The transition from one to the other is discontinuous, particularly in the concentration dependence of the steady-state compliance J_e .²⁵

Experimental Section

Samples. The three-armed samples used were poly- α -methylstyrenes, prepared in a previous work,²² using a trifunctional

Table I
Samples

type	sample no.	$M_w \times 10^{-6}$
star	S-22	0.87 ± 0.04
	S-26	3.57 ± 0.1
linear	α -005	0.44
	α -110	1.19
	α -112	1.82

Table II
Solvents

solvent	temp, °C	η_s , cP	d , g/mL	Θ point
α -chloro-naphthalene	20	2.90	1.194	(good solvent)
	50	1.65	1.168	(good solvent)
n -undecyl anisate	30	15.3	0.974	33 °C
	40	10.7	0.966	33 °C

anionic initiator. The samples used in this work are listed in Table I.

Solvents. A good solvent is α -chloronaphthalene, as used for linear poly- α -methylstyrenes in a previous work.²⁵ α -Chloronaphthalene of the special grade of Katayama Chemical Co. was purified by recrystallization from n -hexane solution at -30 to -40 °C and then by distillation under 10^{-4} mmHg at about 120 °C.

In addition to the good solvent, a Θ solvent was employed in this work. The Θ solvent used in the rheogoniometer must have a high boiling point and low viscosity. To find a Θ solvent for poly- α -methylstyrene, many solvents were examined, and n -undecyl anisate was found to have Θ temperature near room temperature.

n -Undecyl anisate was prepared from 3.5 mol of anisitic acid and 3 mol of n -undecyl alcohol dissolved in 1 L of toluene. The esterification reaction was carried out with concentrated H_2SO_4 at the boiling point of toluene for 10–12 h. The excess acid was extracted with 5% aqueous solution of Na_2SO_3 and then dried with anhydrous sodium carbonate. The n -undecyl anisate was distilled under 10^{-4} mmHg at 140 °C. The Θ temperature of n -undecyl anisate was determined by the Shultz-Flory method,²⁷ as shown in Figure 1. It is about 33 °C.

n -Undecyl anisate and α -chloronaphthalene are convenient for the experiments with the rheogoniometer because of their high boiling points and low volatilities. Their viscosity η_s , density d , and Θ temperature are listed in Table II. The viscosities of the solvents were determined by a capillary viscometer of the Ubbelohde type and their densities by a pycnometer of the Weld type. The purities of these solvents were confirmed by gas chromatography.

Rheological Properties. The measurements of the primary normal stress difference and shear stress of polymer solutions were carried out with a Weissenberg rheogoniometer made by Sanbamo Controls Ltd. Model R-17 equipped with a gap-servo system. The reliability of this instrument was confirmed by comparing the

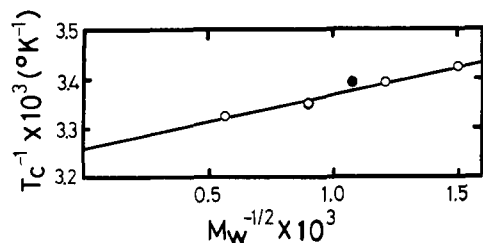


Figure 1. Determination of the Θ temperature for poly- α -methylstyrenes in *n*-undecyl anisate. T_c is the critical temperature determined by the method of Shultz and Flory.²⁷ Open circles show the data of linear polymers, whose molecular weights are 3.16 , 1.24 , 0.68 , and 0.44×10^6 from left to right. The filled circle shows the data for sample S-22.

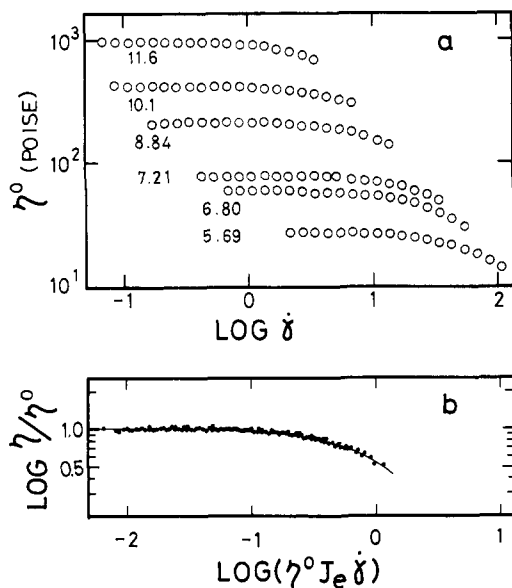


Figure 2. (a) Examples of double logarithmic plots of $\eta(\dot{\gamma})$ vs. $\dot{\gamma}$. Sample, No. S-26 in α -chloronaphthalene at 50°C . Concentrations (g/dL) are shown in the figure. (b) Double logarithmic plot of $(\eta(\dot{\gamma})/\eta^0)$ vs. $(\eta^0 J_e \dot{\gamma})$ for the data in (a). The values of η^0 and J_e are listed in Table III.

primary normal stress differences with the values calculated from shear stress in the linear region, as reported elsewhere.^{28,29} The cone and plate had a 5 cm diameter and a 4° angle. The experiments were carried out mainly at 50°C in α -chloronaphthalene and at 40°C in *n*-undecyl anisate ($\pm 0.1^\circ\text{C}$).

Solutions of about 0.2–0.4 g/dL were prepared by mixing weighted amounts of polymer and solvent at 50°C . For accelerating dissolution, excess cyclohexane was added to the mixtures. The mixtures were gently stirred three times a day by hand until the solution became uniform. After 2 days, cyclohexane was removed by evaporation in a vacuum oven at 50°C . Final polymer concentrations were converted into g/dL, neglecting the volume change in dilution. For measurements with the *n*-undecyl anisate solutions, both the solution and the cone-plate were held at a temperature about 5–10 $^\circ\text{C}$ higher than the experimental temperature and then lowered to the experimental temperature. Experiment was started 20 min after the experimental temperature was attained.

Results

The viscosity coefficient $\eta(\dot{\gamma})$ and primary normal stress coefficient $\psi_{12}(\dot{\gamma})$ are calculated as $P_{21}/\dot{\gamma}$ and $(P_{11} - P_{22})/\dot{\gamma}^2$, respectively, where P_{21} is the shear stress, $P_{11} - P_{22}$ is the primary normal stress difference, and $\dot{\gamma}$ is the shear rate. The zero-shear viscosity η^0 and zero-shear primary normal stress coefficient ψ_{12}^0 were determined by extrapolation to zero shear rate. In concentrated solutions, it is difficult to observe the limiting value of ψ_{12} but the limiting steady-state compliance J_e can be safely determined by

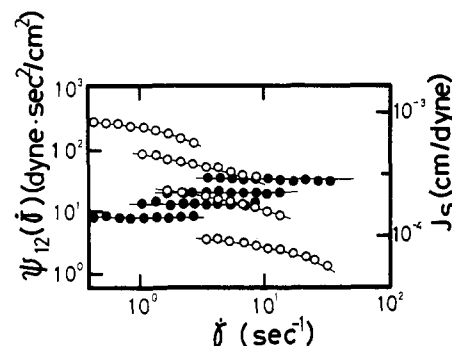


Figure 3. Examples of double logarithmic plots of $\psi_{12}(\dot{\gamma})$ (O) and $J_s(\dot{\gamma})$ (●) vs. $\dot{\gamma}$. Sample, the same as in Figure 2. Concentrations 11.6, 10.1, 8.84, and 7.21 (g/dL) from top to bottom.

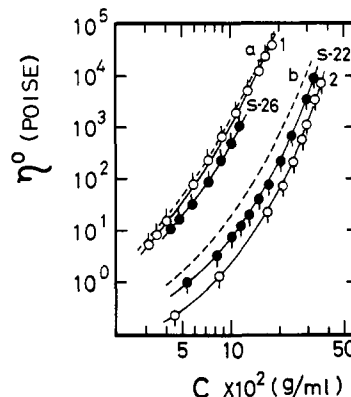


Figure 4. Examples of double logarithmic plots of η^0 vs. C . Open and filled circles show the data of linear and star-shaped poly- α -methylstyrenes, respectively, in α -chloronaphthalene at 50°C . Open circles 1 and 2 show the data for linear polymers with $M_w = 3.3 \times 10^6$ and 4.4×10^6 , respectively. Broken lines a and b show the values estimated for linear polymers with the same molecular weights as S-26 and S-22, respectively. The sample numbers of star-shaped polymers are denoted in the figure.

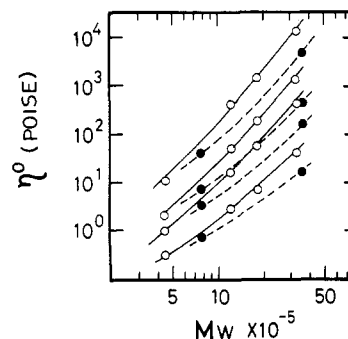


Figure 5. Examples of double logarithmic plots of η^0 vs. M_w . The samples are the same as in Figure 4. Concentrations are 15, 10, 8, and 5 g/dL from top to bottom.

extrapolating J_s defined by eq 1 to zero-shear rate if the molecular weight distribution of the sample is sharp.³⁰

$$J_s(\dot{\gamma}) = (P_{11} - P_{22})/2P_{21}^2 \quad (1)$$

Typical plots of $\eta(\dot{\gamma})$ vs. $\log \dot{\gamma}$ for sample S-26 are shown in Figure 2a. Examples of ψ_{12} and J_s plotted against $\log \dot{\gamma}$ are shown in Figure 3. The zero-shear viscosity η^0 and steady-state compliance J_e can safely be estimated on the graphs. It was reported that plots of $(\eta(\dot{\gamma})/\eta^0)$ vs. $(\eta^0 J_e \dot{\gamma})$ for a given (linear³¹ and branched³²) polymer superpose over a wide range of concentration. The same kind of superposition was also suggested by Sakai et al.²⁵ The superposition of the data in Figures 2a and 3 is also successful as shown in Figure 2b.

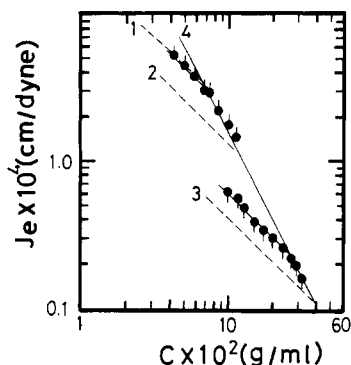


Figure 6. Polymer concentration dependence of J_e in α -chloronaphthalene at 50 °C. Broken lines 1, 2, and 3 show the data of linear poly- α -methylstyrenes with $M_w = 1.82 \times 10^6$, 1.19×10^6 , and 4.4×10^5 , respectively.²⁵ The solid line shows the data of linear polymers in the entanglement region.²⁵ The filled circles (● and ●) show the data of star-shaped polymers S-26 and S-22, respectively.

The η^0 vs. C and also η^0 vs. M_w curves for α -chloronaphthalene solutions of linear and star-shaped poly- α -methylstyrenes are shown in Figures 4 and 5, respectively. In these figures, open circles denote the data of linear polymers reported previously,²⁵ while closed circles denote the data of star-shaped polymers in this work.

The η^0 of star-shaped polymers reveals a concentration dependence similar to that for linear ones, but they have lower values than those of linear polymers with the same molecular weights in both good and poor solvents in this concentration region. In this work, the viscosity enhancement of branched polymers in the higher concentration range reported by previous authors^{15–18} could not be detected.

The limiting steady-state compliance J_e vs. concentration C curves in α -chloronaphthalene solutions at 50 °C are shown in Figure 6. The broken lines are the data of linear poly- α -methylstyrenes in α -chloronaphthalene measured by Sakai et al.²⁵ The filled circles denote the data of S-26 and -22. The concentration dependence of star-shaped polymers appears to be similar to that of linear polymers. Namely, J_e decreases in inverse proportion to concentration in the moderately concentrated region and then decreases in inverse proportion to square concentration in the higher concentration range where intermolecular entanglements are created. The transition between both regions is sharp, in agreement with the results of linear polymers reported previously.²⁵ Moreover, in the moderate concentration range, which is the so-called Rouse region, J_e of the star-shaped polymers are smaller than the values of corresponding linear polymers with the same molecular weights. On the other hand, in the higher concentration region, that is, in the network or entanglement region, J_e of the star-shaped polymers has almost equal values to those of linear polymers. J_e is independent of molecular weight in this concentration region in agreement with the conclusion reported previously.²⁵ The deviation from the inverse square concentration dependence at higher concentrations, reported by previous authors,¹⁸ could not be detected.

Numerical data of η^0 and J_e of star-shaped polymers in α -chloronaphthalene and n -undecyl anisitate and, in addition, numerical data of some linear polymers determined for reference in this work are listed in Table III.

Discussion

Steady-State Compliance. The dependence of J_e on molecular weight and concentration is expressed²⁵ by

$$J_e/M^2 \propto (CM)^\alpha \quad (2)$$

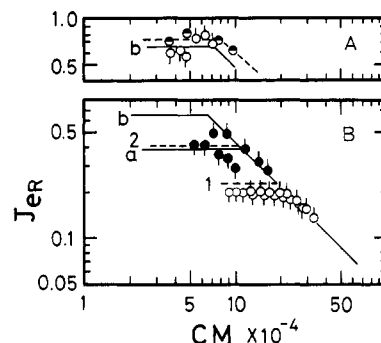


Figure 7. Double logarithmic plots of J_{eR} vs. CM_w . (A) The open circles show the data of linear poly- α -methylstyrenes with $M_w = 1.82 \times 10^6$ (○) and 4.4×10^5 (○) in n -undecyl anisitate at 40 °C. The half-filled circles show the data of linear polystyrenes with $M_w = 6.0 \times 10^5$ in DOP at 30 °C (Θ temperature is 22 °C).³² (B) Solid line a shows the data of linear poly- α -methylstyrenes in α -chloronaphthalene at 50 °C, reported previously,²⁵ while solid line b shows the data in n -undecyl anisitate at 40 °C, determined in (A). Broken lines 1 and 2 denote the values estimated from eq 7 for star-shaped polymers in α -chloronaphthalene and n -undecyl anisitate, respectively. Circles ○ and ◐ denote the experimental data of J_e for star-shaped polymers S-26 and S-22 in α -chloronaphthalene, respectively, while ● and ◐ denote their data in n -undecyl anisitate, respectively.

where the constant is $\alpha = -1$ and -2 in the Rouse and entanglement regions, respectively. It may be convenient for further discussions to use the reduced steady-state compliance J_{eR} ²

$$J_{eR} = \left(\frac{J_e CRT}{M} \right) \left(\frac{\eta^0}{\eta^0 - \eta_s} \right)^2 \quad (3)$$

where η^0 and η_s are the zero-shear viscosities of the solution and the solvent, respectively.

For infinitely dilute solutions,¹ the limiting reduced steady-state compliance J_{eR}^0 is related to the ratio of relaxation times such as

$$J_{eR}^0 = \lim_{c \rightarrow 0} \left(\frac{RT}{M[\eta]^2} \frac{J_e}{c} \right) = \frac{\sum \tau_i^2}{(\sum \tau_i)^2} \quad (4)$$

where τ_i is the i th relaxation time. For solutions of linear polymer, the molecular theories of Rouse³ and Zimm⁵ predict

$$J_{eR}^0 = 0.4 \quad \text{if draining} \quad (5a)$$

$$J_{eR}^0 = 0.206 \quad \text{if nondraining} \quad (5b)$$

At the limit of infinite dilution, it was shown¹ that the dynamic properties of monodisperse linear polymer solutions can be explained well by the theory of Zimm⁵ with the model of nondraining coils.

In moderately concentrated solutions, that is, in the Rouse region, it was reported^{2,23,25,30} that J_{eR} is about 0.4, and appears to be insensitive to polymer concentration. However, it is to be noted that this value of J_{eR} was obtained in good solvents. In Θ solvents such as DOP for polystyrene and n -undecyl anisitate for poly- α -methylstyrene, J_{eR} in moderately concentrated solutions is much higher than this value and is found to be about 0.7. The data of linear polystyrenes in DOP and those of linear poly- α -methylstyrenes in n -undecyl anisitate are shown in Figure 7A. It is certainly significant that J_e in the Rouse region is proportional to (M/C) , that is, J_{eR} is a constant. However, the absolute value may have no significance in the moderately concentrated solutions.

Table III
Steady-Flow Viscosity and Compliance at Zero Rate of Shear

sample	solvent	temp, ±0.1 °C	$C \times 10^2$, g/mL at 50 °C	η^0 , P	J_e , cm/dyn
S-26	α -chloronaphthalene	50	11.6	9.60×10^2	1.46×10^{-4}
		50	10.1	4.25×10^2	1.80×10^{-4}
		50	8.84	2.21×10^2	2.29×10^{-4}
		50	7.21	7.90×10	3.00×10^{-4}
		50	6.80	6.05×10	3.10×10^{-4}
		20	5.69	5.80×10	4.33×10^{-4}
		50	5.69	2.70×10	3.87×10^{-4}
		20	4.94	3.15×10	5.10×10^{-4}
		20	4.32	1.94×10	5.76×10^{-4}
S-22	α -chloronaphthalene	50	31.8	8.90×10^3	1.60×10^{-5}
		50	29.1	3.40×10^3	2.01×10^{-5}
		50	26.4	1.46×10^3	2.20×10^{-5}
		50	23.7	6.39×10^2	2.60×10^{-5}
		50	20.0	2.20×10^2	3.03×10^{-5}
		50	16.9	7.80×10	3.40×10^{-5}
		50	14.7	4.00×10	3.80×10^{-5}
		50	12.9	2.20×10	5.00×10^{-5}
		20	12.9	5.83×10	5.60×10^{-5}
		20	11.5	3.31×10	6.20×10^{-5}
		20	10.3	2.06×10	6.90×10^{-5}
		20	8.05	7.77×10	
		20	5.31	2.30×10	
sample	solvent	temp, ±0.1 °C	$C \times 10$, g/mL at 40 °C	η^0 , P	J_e , cm/dyn
S-26	<i>n</i> -undecyl anisitate	40	5.85	1.37×10^3	5.25×10^{-4}
		40	4.87	4.65×10^2	7.80×10^{-4}
		40	3.88	1.21×10^2	1.15×10^{-3}
		40	2.91	2.50×10^1	1.95×10^{-3}
		40	2.42	9.30×10^0	2.32×10^{-3}
S-22	<i>n</i> -undecyl anisitate	40	11.8	7.50×10^2	8.00×10^{-5}
		40	10.3	2.95×10^2	1.05×10^{-4}
		40	8.78	1.12×10^2	1.27×10^{-4}
		40	7.32	4.30×10^1	1.88×10^{-4}
		40	6.32	2.18×10^1	2.10×10^{-4}
α -112	<i>n</i> -undecyl anisitate	40	3.89	4.23×10^1	1.20×10^{-3}
		40	3.41	1.45×10^1	1.60×10^{-3}
		40	2.91	6.40×10^0	1.73×10^{-3}
α -005	<i>n</i> -undecyl anisitate	40	10.3	6.10×10^1	8.80×10^{-5}
		40	9.28	3.20×10^1	1.12×10^{-4}
		40	8.29	1.93×10^1	1.17×10^{-4}

In the infinitely dilute solutions of star-shaped polymers, it can be shown from the theory of Zimm and Kilb¹² that

$$J_{eR}^0 = 0.4 \frac{(15f - 14)}{(3f - 2)^2} \quad \text{if draining} \quad (6a)$$

$$J_{eR}^0 = 0.2 \frac{(31.8f - 28.2)}{(3.90f - 1.94)^2} \quad \text{if nondraining} \quad (6b)$$

where f is the degree of branching. If $f = 3$, we have $J_{eR}^0 = 0.25$ and 0.14 for the free-draining and nondraining cases, respectively. Ham¹¹ and Chompff¹⁴ numerically gave the same values for J_{eR}^0 as Zimm and Kilb, in the draining case.

In the Rouse region, therefore, it may be reasonable to predict that

$$(J_{eR})_b = (J_{eR})_l g_J \quad (7)$$

where the subscripts l and b denote the linear and star-shaped polymers, and

$$g_J = (15f - 14)/(3f - 2)^2 \quad \text{if draining} \quad (8a)$$

$$g_J = (31.8f - 28.2)/(3.90f - 19.4)^2 \quad \text{if nondraining} \quad (8b)$$

$(J_{eR})_l$ may vary with solvent, temperature, etc., but the relationship in (11) may be valid independent of solvent

and temperature, though, strictly speaking, the theory of Zimm and Kilb is valid only in Θ solvents. In the case of $f = 3$, g_J gives almost identical values, 0.7 and 0.61, respectively.

No theoretical prediction of J_{eR} of branched polymers in the entanglement region has been given. However, it is reasonable to predict that J_e is independent of molecular weight and branching if the molecules make a quasi-network. That is, J_{eR} may be proportional to $(CM)^{-1}$ and coincide with the data of linear polymers.

For the comparison between the above predictions and experiments, double logarithmic plots of J_{eR} vs. CM are shown in Figure 7B. The solid lines a and b show the data for linear poly- α -methylstyrenes²⁵ in α -chloronaphthalene (good solvent) and *n*-undecyl anisitate (Θ solvent), respectively. The open and filled circles are the data of star-shaped polymers in α -chloronaphthalene and in *n*-undecyl anisitate, respectively. It is clear that J_{eR} for star-shaped polymers is lower than that for linear polymers in both Θ and good solvents. The broken lines 1 and 2 show the values for star-shaped polymers in Θ and good solvents predicted from eq 11 ($g_J = 0.65$ is assumed), respectively. The agreement between the experimental and predicted values is satisfactory in both Θ and good solvents. The data of two samples do not superpose in the Θ solvent. The reproducibility of measurements in Θ solvents is not as high as in good solvents; however, we do

not discuss the problem in this paper.

In conclusion, the steady-state compliance of star-shaped polymers is lower than that of the corresponding linear polymers with the same molecular weights in moderately concentrated solutions, but it is independent of molecular weight and branching in the entanglement region. This conclusion is opposite to the conclusion obtained for branched polymers having many more branches in the undiluted state.¹⁹⁻²¹ The experimental results of rheo-goniometry with those highly branched samples and the reason for the discrepancy will be discussed in a following paper.

Zero-Shear Viscosity. The transition from the Rouse region to the entanglement region is not as clear in viscosity as in the steady-state compliance, since the viscosity is enhanced due to the effect of entanglement even in the Rouse region. The entanglement region may be defined if η^0 is proportional to the 3.4th power of molecular weight.

If the polymer chains are entangled enough, the ratio of the zero-shear viscosities of star-shaped (η_b^0) and corresponding linear (η_l^0) polymers with the same molecular weight at the same polymer concentration was calculated by Bueche,¹³

$$\eta_b^0/\eta_l^0 = g_s^{7/2} \quad (9)$$

where g_s is defined by the ratio of unperturbed radii of gyration of star-shaped and linear polymers with the same molecular weight and is given by

$$g_s (\equiv \langle S_0^2 \rangle_b / \langle S_0^2 \rangle_l) = (3f - 2)/f^2$$

Alternatively Graessley⁶ presented the following equation for the zero-shear viscosity of linear polymers,

$$\eta_l^0 = K \langle S^2 \rangle_l [1 + 0.131(M/M_e)^{2.5}] \quad (10)$$

where K is a constant and M_e is the molecular weight between two adjacent entanglement points. The theory of Graessley was extended¹⁹ to the viscosity of branched polymers

$$\eta_b^0 = K \langle S^2 \rangle_b [1 + 0.743(M_b/M_e)^{2.5}] \quad (11)^{33}$$

where M_b is the molecular weight of a branch. If there are enough entanglement points in a molecule or in a branch, we may neglect unity in comparison with the last terms in eq 14 and 15, so that we may have

$$\eta_b^0/\eta_l^0 = 5.67g_s(1/f)^{2.5} \quad (12)$$

Equations 13 and 16 imply that $\log \eta^0$ vs. $\log C$ plots in Figure 4 for linear and star-shaped polymers with the same molecular weight must be parallel and the difference between them must be

$$\log (\eta_b^0/\eta_l^0) = -0.382 \quad \text{from eq 13} \quad (13a)$$

$$\log (\eta_b^0/\eta_l^0) = -0.548 \quad \text{from eq 16} \quad (13b)$$

in the case of $f = 3$.

The experimental data in Figure 4 show that the above prediction is quantitatively correct. That is, $\log \eta_b^0$ vs. $\log C$ plots of star-shaped polymers are parallel to those of linear polymers. The experimental value of $\log (\eta_b^0/\eta_l^0)$ estimated from the figure is about 0.5.

The molecular weight dependence of linear and branched polymers may be more complicated. If the linear polymers are entangled enough, the zero-shear viscosities of linear polymers may be determined by the entanglement number per polymer chain, which is proportional to CM .^{2,34} That is, the molecular and concentration dependence of

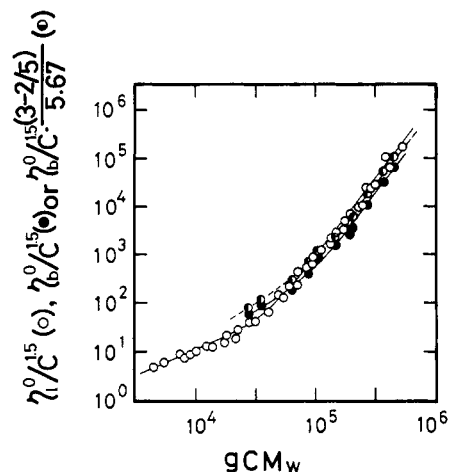


Figure 8. Plots of zero-shear viscosity data of star-shaped polymers in the forms of eq 15 (●) and eq 16 (○). Open circles (○) denote the data for linear polymers in α -chloronaphthalene at 50 °C. Experimental conditions are explained in Figure 4.

zero-shear viscosity of linear polymers can be empirically expressed by the following equation^{2,18,26}

$$\eta_l^0 = K_1(\xi, T) C^a F(CM) \quad (14)$$

where ξ and T are the frictional coefficient of a polymer segment and temperature, respectively, and a is a constant, about 1.5–2. It was shown by Graessley¹⁸ that $\eta^0/C^{1.5}$ can be expressed by a universal function, CM . It was confirmed as seen in Figure 8 that our previous data of linear poly- α -methylstyrenes can also be expressed by eq 14.

Extension of eq 14 to η^0 of branched polymers was also done by Graessley.¹⁸ His equation is

$$\eta_b^0 = K_1(\xi, T) C^a F(g_s CM) \quad (15)$$

where η_b^0 is the zero-shear viscosity of branched polymers. Since $F(CM)$ in eq 14 is proportional to $(CM)^{3.4}$ in the range of high (CM) , combination of eq 9 and 14 gives eq 15. On the other hand, combination of eq 12 and 14 gives

$$\eta_b^0[(3 - 2/f)^{2.5}/5.67] = K_1(\xi, T) C^a F(g_s CM) \quad (16)$$

The present experimental data of η_b^0 are plotted in the form of eq 15 and 16 in Figure 8. If the above predictions are correct, either the plot in the form of eq 15 or eq 16 should fit the curve for linear polymers. The agreement between both data for linear and branched polymers is fairly good but the deviation may be beyond the experimental error. Previous authors¹⁸ found much greater disagreement between eq 15 and their own experimental data.

References and Notes

- (1) J. D. Ferry, "Viscoelastic Properties of Polymers", Wiley, New York, N.Y., 1970.
- (2) W. W. Graessley, *Adv. Polym. Sci.*, **16**, 1 (1974).
- (3) P. E. Rouse, *J. Chem. Phys.*, **21**, 1272 (1953).
- (4) F. Bueche, *J. Chem. Phys.*, **22**, 1570 (1974).
- (5) B. Zimm, *J. Chem. Phys.*, **24**, 269 (1956).
- (6) W. W. Graessley, *J. Chem. Phys.*, **43**, 2696 (1965); **47**, 1942 (1967).
- (7) A. J. Chompff and J. A. Duizer, *J. Chem. Phys.*, **45**, 1505 (1966).
- (8) A. J. Chompff and W. Prins, *J. Chem. Phys.*, **48**, 235 (1968).
- (9) W. W. Graessley, *J. Chem. Phys.*, **54**, 5143 (1971).
- (10) P. A. Small, *Adv. Polym. Sci.*, **18**, 1 (1975).
- (11) J. S. Ham, *J. Chem. Phys.*, **26**, 625 (1957).
- (12) B. H. Zimm and R. W. Kilb, *J. Polym. Sci.*, **37**, 19 (1959).
- (13) F. Bueche, *J. Chem. Phys.*, **40**, 484 (1964).
- (14) A. J. Chompff, *J. Chem. Phys.*, **53**, 1566, 1577 (1970).
- (15) G. Kraus and J. T. Gruver, *J. Polym. Sci., Part A*, **3**, 105 (1965).
- (16) R. A. Mendelson, W. A. Bowles, and F. L. Finger, *J. Polym. Sci., Part A-2*, **8**, 455 (1970).
- (17) R. P. Chartoff and B. Mazwell, *J. Polym. Sci., Part A-2*, **8**, 455 (1970).

- (18) W. W. Graessley, T. Masuda, J. E. L. Roovers, and N. Hadjichristidis, *Macromolecules*, **9**, 127 (1976).
- (19) T. Fujimoto, H. Narukawa, and M. Nagasawa, *Macromolecules*, **3**, 57 (1970).
- (20) T. Fujimoto, H. Kajiura, M. Hirose, and M. Nagasawa, *Polym. J.*, **3**, 181 (1972).
- (21) T. Masuda, Y. Ohta, and S. Onogi, *Macromolecules*, **4**, 763 (1971).
- (22) T. Fujimoto, S. Tani, K. Takano, M. Ogawa, and M. Nagasawa, *Macromolecules*, in press.
- (23) W. W. Graessley and L. Segal, *Macromolecules*, **2**, 49 (1969).
- (24) Y. Einaga, K. Osaki, M. Kurata, and M. Tamura, *Macromolecules*, **4**, 87 (1971).
- (25) M. Sakai, T. Fujimoto, and M. Nagasawa, *Macromolecules*, **5**, 786 (1972).
- (26) G. C. Berry and T. G. Fox, *Adv. Polym. Sci.*, **5**, 261 (1968).
- (27) A. R. Shultz and P. J. Flory, *J. Am. Chem. Soc.*, **74**, 4760 (1952).
- (28) H. Endo and M. Nagasawa, *J. Polym. Sci. Part A-2*, **8**, 371 (1970).
- (29) J. Kajiura, H. Endo, and M. Nagasawa, *J. Polym. Sci., Polym. Phys. Ed.*, **11**, 2371 (1973).
- (30) H. Endo, T. Fujimoto, and M. Nagasawa, *J. Polym. Sci., Part A-2*, **9**, 345 (1971).
- (31) G. C. Berry, B. L. Hager, and C.-P. Wong, *Macromolecules*, **10**, 361 (1977).
- (32) G. C. Berry, *J. Chem. Phys.*, **46**, 1338 (1967).
- (33) The constant (0.305) in eq 8 of ref 19 should be corrected to 0.743.
- (34) F. Bueche, *J. Chem. Phys.*, **25**, 599 (1956).

Star-Branched Polymers. 2. The Reaction of Dienyllithium Chains with the Isomers of Divinylbenzene

R. N. Young¹ and L. J. Fetters*

*Institute of Polymer Science, The University of Akron, Akron, Ohio 44325.
Received April 3, 1978*

ABSTRACT: The crossover and subsequent homopolymerization reactions of *m*- and *p*-divinylbenzene with butadienyl- and isoprenyllithium in benzene have been followed by UV spectroscopy. The *p*-divinylbenzene was found to react slightly faster with the dienyllithium chain ends than the meta isomer. Nonetheless, *m*-divinylbenzene was found to be more effective than the para form in linking the dienyllithium chains into the star-branched architecture, i.e., at a given DVB/RLi ratio the meta isomer yielded a higher extent of branching than did the para form.

Star-branched polystyrene–polydiene block copolymers and polyisoprene homopolymers containing up to 56 weight-average number of arms have been synthesized^{2–5} using divinylbenzene as the linking agent. This procedure involved the addition of the divinylbenzene to the solution of polydienyllithium chains after the diene monomer has been consumed. Thus, the polymerization of divinylbenzene formed the microgel nucleus of these star-shaped polymers, a procedure adumbrated by Milkovich in 1965.⁶ Rempp and co-workers^{7–12} were the first to successfully exploit this concept, in this case with regard to the synthesis of star-branched polystyrenes. The arms of these star species possessed narrow molecular weight distributions as a result of the termination free aspect¹³ of diene and styrene polymerizations initiated by organolithium species in hydrocarbon solvents.

An examination of the rheological properties of these star-branched block and homopolymers^{2,4} in the melt state has shown that viscosity is *independent* of the extent of branching and depends only on arm molecular weight. In view of this, and the interesting and unexpected dilute solution properties and chain dimensions of these star-shaped polymers,^{4,5} it was deemed of interest to investigate the star formation process involving the reaction between the dienyllithium chain ends and the divinylbenzene isomers. The formation of a star polymer by the reaction of divinylbenzene would be anticipated to be kinetically and mechanistically a complex reaction requiring the participation of several simultaneous and competitive steps. This process was followed by UV spectroscopy using benzene as the solvent and oligomeric dienyllithium chains.

Experimental Section

These anionic polymerizations involved the purification prior to use of monomers, solvent, the divinylbenzene isomers and all glassware equipment. All purifications and polymerizations were conducted under high vacuum (10^{-6} Torr) using the procedures described elsewhere.^{2,14} The initiator was *sec*-butyllithium which was purified by distillation under vacuum conditions. The re-

sulting benzene solutions of the initiator were colorless.

The *m*-, *p*-divinylbenzene mixture was obtained from Chemical Samples. The analysis (as outlined below) of this mixture showed that it was 93% divinylbenzene with a meta–para ratio of 3/1. The major impurities were the ethylvinylbenzene isomers. The *m*-divinylbenzene was obtained from Haven Chemical while the para isomer was separated from a commercial mixture (Foster-Grant 80% divinylbenzene) by the complexation with cuprous chloride^{15–18} at 0 °C followed by heating. The *p*-divinylbenzene was then further purified by crystallization from methanol. Worsfold¹⁹ has also used this separation technique successfully. For run 28a the para isomer was obtained from the meta and para mixture from Chemical Samples. Analysis of the two isomers by IR, 300 MHz ¹H NMR, ¹³C NMR, gas chromatography, and mass chromatography showed that each isomer was >95% pure. The major impurity in each species was the other isomer with only trace amounts of the ethylvinylbenzene species present. Following purification, the divinylbenzene isomers were diluted with benzene to give 5–10% (v/v) solutions. These were stored in ampules under high vacuum at –20 °C until use. Our experience has shown that divinylbenzene solutions of this concentration can be stored at this temperature for at least 1 year without the loss of vinyl groups through dimerization or polymerization.

The poly(dienyl)lithium chains were made by reacting a dilute monomer–benzene solution with *sec*-butyllithium. Reaction periods of 72 to 96 h at room temperature were used in order to ensure that no diene remained. These solutions were cooled several times in order to draw into solution residual diene existing in the void volume of the reactor. These reaction mixtures were then divided into ampules and stored at –20 °C until use. Parenthetically, it should be noted that NMR and UV analysis by numerous workers has shown that these dienyllithium chain ends undergo no transformations, e.g., isomerization or lithium hydride elimination, under the conditions used in this work for their preparation. Thus, in hydrocarbon solvents these allylic lithium species exhibit the degree of stability necessary for general mechanistic evaluations. This is not the case for the allylic sodium or potassium species^{20,21} or for the “dicarbanionic tetramer” of α -methylstyrene involving either of these two counterions. This initiator has been shown to be unstable,^{22–24} particularly under the influence of white light and UV radiant energy.²⁴

The UV spectroscopic measurements were carried out at 21